available at www.sciencedirect.com

ScienceDirect

journal homepage: www.elsevier.com/locate/ejps

Dimethoxyaurones: Potent inhibitors of ABCG2 (breast cancer resistance protein)

*Hong-May Sim, Chong-Yew Lee, Pui Lai Rachel Ee, Mei-Lin Go**

Department of Pharmacy, National University of Singapore, 18 Science Drive 4, Singapore 117543, Singapore

ARTICLE INFO

Article history:
Received 28 May 2008
Received in revised form
10 July 2008
Accepted 24 July 2008
Published on line 3 August 2008

Keywords:
4,6-Dimethoxyaurones
Modulators
ABCG2
ABCB1
Antiproliferative activity
Structure–activity relationship

ABSTRACT

A series of 4,6-dimethoxyaurones were synthesized by reacting 4,6-dimethoxybenzofuran-3(2*H*)-one with various benzaldehydes in a base-catalyzed aldol reaction. A Z configuration was assigned to the aurones based on spectroscopic and crystallographic data. The aurones were tested for their ability to modulate ABCG2 (breast cancer resistance protein)-mediated multidrug resistance in vitro. Several members (0.5 μM) increased the accumulation of mitoxantrone (MX) in human breast cancer cells (MDA-MB-231) transfected with ABCG2 and re-sensitized these cells to the cytotoxic effects of MX. In the re-sensitization assay, aurones at 0.5 μM reduced the resistance of the transfected cells to MX to just twice that of the parental cells, exceeding fumitremorgin C (FTC) tested at the same concentration. The aurones (10 μM) also increased calcein-AM accumulation in MDCKII/MDR1 cells that were transfected with ABCB1 (P-glycoprotein), at levels comparable to verapamil tested at the same concentration. Structure–activity analysis showed that substitution of the benzylidene ring B of the aurone template was less important for ABCG2 inhibition, with little variation in activity noted for compounds with an unsubstituted ring B or one that was substituted. In contrast, substitution of ring B gave rise to better inhibitors of ABCB1. A preference for the 3′ position of ring B was noted. There was also some indication from the data that aurones with good ABCG2 inhibitory activity were poor ABCB1 inhibitors and vice versa, but further confirmation would be required. Limited antiproliferative activity (>70% cell survival) was observed for many aurones on four different cell lines. Thus, functionalized 4,6-dimethoxyaurones are promising ABCG2 inhibitors that combine good activity at submicromolar concentrations with limited antiproliferative activity.

1. Introduction

One of the major obstacles to effective cancer chemotherapy is the acquisition of multidrug resistance (MDR) by cancer cells (Szakács et al., 2006; Shukla et al., 2008). This phenomenon is commonly associated with the overexpression of ATP-binding cassette (ABC) transporters, of which ABCB1 (P-glycoprotein, Pgp), ABCC1 (MRP1), and ABCG2 (breast cancer resistance protein, BCRP) are the most relevant in the clinical setting. These transporters actively extrude a broad panel of therapeutically useful cytotoxic drugs, suppressing their intracellular levels to below cell-killing thresholds, thus resulting in treatment failures and poor patient outcomes. Various strategies have been proposed to circumvent this problem and these may be broadly classified as those involved in the co-administration of transporter inhibitors and cytotoxic agents

* *Corresponding author at*: Department of Pharmacy, Faculty of Science, National University of Singapore, 18 Science Drive 4, Singapore 117543, Singapore. Tel.: +65 6516 2654; fax: +65 6779 1554.
E-mail address: phagoml@nus.edu.sg (M.-L. Go).
0928-0987/$ – see front matter © 2008 Elsevier B.V. All rights reserved.
doi:10.1016/j.ejps.2008.07.008

("engage"), discovering and developing cytotoxic drugs that bypass transporter-mediated efflux ("evade"), and "exploiting" the paradoxical sensitivity of MDR cells (Szakács et al., 2006). The first approach of developing clinical inhibitors of ABC transporters has been vigorously pursued but has not resulted in a suitable clinical candidate (Robert and Jarry, 2003; Breedveld et al., 2006).

Aurones (2-benzylidenebenzofuran-3(2*H*)-ones) are a group of lesser known flavonoids that are structural isomers of flavones. They impart a golden yellow color to flowers and may function as phytoalexins in plants (Pare et al., 1991). In contrast to flavonoids, there are relatively few reports on the biological properties of aurones. A review cited their potential in cancer chemotherapy, as agents for the treatment of parasitic and microbial infections, and as inhibitors of an enzyme involved in the metabolism of thyroid hormones (Boumendjel, 2003). They have also been reported to be antiproliferative agents interfering with G2/M phase of the cell cycle (Lawrence et al., 2003), tyrosinase inhibitors (Okombi et al., 2006) and as potentially useful imaging agents for detecting β-amyloid plaques in Alzheimer's disease (Ono et al., 2007). Several reports have focused on aurones as modulators of Pgp-mediated multidrug resistance (Boumendjel et al., 2002a; Boumendjel, 2003; Hadjeri et al., 2003; Václavíková et al., 2006). The inhibitory activity was ascribed to the structural mimicry between the benzofuranone ring of the aurone and the adenine of ATP (Boumendjel, 2003). Support for this hypothesis came from a study that demonstrated the binding of aurones to the cytosolic nucleotide binding domain of mouse Pgp (Boumendjel et al., 2002a). The same mimicry has been proposed for the chromenone ring of flavones, but when compared with other flavonoids, aurones showed greater binding affinity and more potent activity as Pgp modulators (Boumendjel, 2003; Hadjeri et al., 2003; Václavíková et al., 2006). This led to the proposal that the conformationally restrained aurone template may have a better fit in the ATP-binding site of the transporter (Boumendjel, 2003).

Some of the shortcomings of flavonoids as modulators of ABC transporters are their moderate potencies and their broad spectrum of biological activities (Boumendjel et al., 2002b). In this respect, the greater potencies reported for aurones may be an advantage. On the other hand, a functionalized 4,6-dihydroxyaurone was reported to have a good docking fit in the ATP-binding site of CDK2 (Schoepfer et al., 2002). This finding implied that aurones may have affinities for the same site in other kinases and related proteins. If so, they would have a broader spectrum of activities than presently reported. Although there are several reports on the Pgp modulatory activity of aurones, the structural variations made to the template has been quite limited (Boumendjel et al., 2002a,b; Boumendjel, 2003; Hadjeri et al., 2003; Václavíková et al., 2006). Moreover, little is known of how aurones affect ABCG2, a clinically relevant ABC transporter that is known to interact with flavonoids (S. Zhang et al., 2005). With this background in mind, we prepared a series of 15 4,6-dimethoxyaurones with different substituents on ring B. Our objectives are to evaluate their potential as inhibitors of ABCG2, and to assess the structure–activity relationships associated with these modifications. Our investigations involved evaluating the compounds for their abilities to increase mitoxantrone (MX) accumulation in human breast cancer cells (MDA-MB-231) transfected with the human wild type (482R) BCRP cDNA, and to re-sensitize these cells to the cytotoxic effects of MX. To assess the selectivity of these aurones for ABCG2, their effects on the ABCB1 transporter were investigated by the calcein-AM accumulation assay with MDCKII cells transfected with human MDR1 cDNA. Finally, antiproliferative activities were evaluated by the MTT assay on several cell lines.

2. Materials and methods

2.1. *Synthesis of aurone library: general details*

Reagents (synthetic grade or better) for the synthesis of the aurones were obtained from Sigma–Aldrich Chemical Company Inc. (St. Louis, MO, USA) and used without further purification. Melting points were measured on a Gallenkamp melting point apparatus and reported as uncorrected values. Mass spectra were captured on an LCQ Finnigan MAT fitted with a chemical ionization (APCI probe) and *m*/*z* ratios for the molecular ion were reported. ^{1}H and ^{13}C NMR spectra were determined on a Bruker-Spectrospin 300 Ultrashield spectrometer and referenced to TMS. Infrared spectra were collected on solid KBr disks using a Perkin Elmer Precisely Spectrum 100 FT-IR Spectrometer. Thin layer chromatography was carried out on Merck Silica 60 F254 plates. Flash chromatography was carried out using Merck silica gel, 0.040–0.063 mm. The purity of final compounds were verified by combustion analysis (C,H) on a Perkin-Elmer PE 2400 Elemental Analyzer and by high pressure liquid chromatography (HPLC) for compound **14**.

2.1.1. *3,5-Dimethoxyphenoxyacetic acid (**16**)*

The method of Lawrence et al. (2003) was followed. To a solution of 3,5-dimethoxyphenol (0.83 g, 5.44 mmol) in anhydrous DMF (10 ml) was added sodium hydride (0.33 g, 13.6 mmol). Chloroacetic acid (0.51 g, 5.44 mmol) in DMF (10 ml) was added dropwise and the mixture stirred under cover of nitrogen gas at room temperature for 12 h. After this time, the mixture was quenched with 4 M HCl (100 ml) and extracted with dichloromethane (3× 50 ml). The organic phase was washed with brine, dried with anhydrous Na_2SO_4 and evaporated *in vacuo* to give brownish oil which solidified to a white solid on cooling in an ice-bath. Recrystallisation in chloroform–hexane gave **16** in 76% yield. White needle-like crystalline solid; mp 148–149 °C; ^{1}H NMR ($CDCl_3$, 300 MHz): δ 6.14 (t, 1H, J = 2.0 Hz), 6.11 (d, 2H, J = 2.1 Hz), 4.65 (s, 2H), 3.74 (s, 6H); MS (APCI) *m*/*z* $[M+1]^+$ 212.5.

2.1.2. *4,6-Dimethoxybenzofuran-3(2H)-one (**17**)*

The method of Lawrence et al. (2003) was followed. 20 g of polyphosphoric acid was heated to 80 °C after which was added 0.5 g of compound **16**. The mixture was stirred at 90 °C for 8 h and then poured into ice-water (100 ml) and subsequently extracted with dichloromethane (4× 50 ml). The combined organic phase was washed with brine, dried with anhydrous Na_2SO_4 and evaporated *in vacuo*. The residue

was purified by column chromatography, with hexane:ethyl acetate 2:1 as eluting solvent. **17** was obtained as a pale yellow solid, yield: 56%; mp 137–139 °C; ^{1}H NMR ($CDCl_3$, 300 MHz): δ 6.16 (d, 1H, J = 1.5 Hz), 6.02 (d, 1H, J = 1.1 Hz), 4.60 (s, 2H), 3.91 (s, 3H), 3.87 (s, 3H); MS (APCI) m/z $[M+1]^+$ 195.1.

2.1.3. *General procedure for the synthesis of aurones*

The method of Lawrence et al. (2003) was followed. To a solution of **17** (100 mg, 0.52 mmol) in methanol (10 ml) was added the substituted benzaldehyde (0.76 mmol), followed by a solution of KOH (500 mg, 8.92 mmol) in distilled water (1 ml). The solution was stirred at room temperature for 1–3 h. The desired compound was obtained as a precipitate, removed by suction filtration, washed with cold methanol and crystallized in ethanol or methanol to give the purified aurone (**1–15**). In the case of aurones **6** and **7**, additional protection and deprotection of the phenolic hydroxyl group on the benzaldehyde were required. Spectroscopic and other analytical details of aurones **1–15** are given in Supplementary Information.

2.1.4. *Protection and deprotection of phenolic hydroxyl groups on benzaldehydes for syntheses of aurones **6** and **7***

3-Hydroxybenzaldehyde or 4-hydroxylbenzaldehyde (3 mmol), pyridinium *p*-toluenesulphonate (50 mg, 0.2 mmol) and 3,4-dihydro-2*H*-pyran (673 mg, 8 mmol) were dissolved in dichloromethane (10 ml) and stirred for 4 h at room temperature. The reaction mixture was then washed with 1 M Na_2CO_3 (3× 20 ml). The organic layer was dried over anhydrous Na_2SO_4 and concentrated *in vacuo* to give the crude tetrahydropyranyl ether (**18**) as a yellow oil which was used without purification for the condensation reaction with **17** as described in Section 2.1.3. After the period of stirring, the reaction mixture was acidified with 4 M HCl, stirred for 4 h at room temperature, and filtered under vacuum to give the crude product (**6**, **7**) which was recrystallized from methanol.

2.2. *Materials for biological assays*

Mitoxantrone (MX), fumitremorgin C (FTC), calcein acetoxymethyl ester (calcein-AM), verapamil, cyclosporin A, 3-(4,5-dimethylthiazol-2-yl)-2,5-diphenyltetrazolium bromide (MTT) were purchased from Sigma–Aldrich, St. Louis, MO, USA. The breast cancer cell line, MDA-MB-231, stably transfected with expression vectors for wild type 482R BCRP (R cells) and pcDNA3.1 (parental V cells) were kindly provided by Dr. Douglas D. Ross (Greenebaum Cancer Center, University of Maryland, Baltimore, USA). Both MDA-MB-231/V and MDA-MB-231/R cells were cultured in 75-cm^3 flasks with RPMI 1640 (Invitrogen Corporation, CA, USA) culture media supplemented with 10% fetal bovine serum (Hyclone, UT, USA) at 37 °C in a 5% CO_2 humidified atmosphere. The culture media contained 0.1 mg/ml streptomycin sulfate and 0.1 mg/ml penicillin G (Sigma Chemical Co., St. Louis, MO, USA) and 1.0 mg/ml geneticin (Invitrogen Corporation, CA, USA). Mardin-Darby canine kidney (MDCK) cells transfected with the expression vector for human mdr1 cDNA was a gift from Dr. Anton Berns (Netherlands Cancer Institute, Antoni van Leeuwenhoek Hospital, Amsterdam, Netherlands). The cells were grown in DMEM medium containing 10% fetal bovine serum and 0.1 mg/ml streptomycin sulfate and penicillin G. Human colon carcinoma HCT116 and normal human diploid embryonic lung fibroblasts CCL-186 were purchased from American Type Culture Collection (Rockville, MD). HCT116 cells were cultured in McCoy's 5A modified medium supplemented with 10% FBS, 0.1% penicillin G and 0.1% streptomycin. CCL-186 cells were grown in Eagle's minimal essential medium (EMEM) supplemented with 10% FBS, 0.3% L-glutamine, 0.1% penicillin G and 0.1% streptomycin. All the cells were sub-cultured when they reached 80–90% confluency and used within 10 passages for the assays.

2.3. *Western blot analysis*

Fifteen microgram of cell lysates from MDA-MB-231 (R and V cells), and 40 μg of cell lysates from MDCKII (wild type) and MDCKII/MDR1 were subjected to electrophoresis on 7.5% sodium dodecyl sulphate-polyacrylamide gel (SDS-PAGE) and transferred to nitrocellulose membranes (Bio-Rad Laboratories Pte Ltd., Singapore) for overnight blocking at room temperature. The blots were probed with primary antibodies followed by horseradish peroxidase-conjugated anti-mouse secondary antibody. The primary antibodies used were anti-BCRP (BXP-21), anti-Pgp (C219), anti-MRP1 (MRPr-1) and anti-MRP2 (M2III-6). The blots were washed and incubated with West Femto luminal/enhancer solution (Pierce Chemicals, Rockford, IL) and stable peroxide solution for 5 min. The membranes were analyzed with FluorChemTM 9900 (Alpha Innotech Corporation, San Leandro, CA).

2.4. *Mitoxantrone accumulation studies*

The accumulation of MX was determined by flow cytometry on MDA-MB-231/R and MDA-MB-231/V cells by a previously described method (Minderman et al., 2002). Stock solutions of aurones, MX and FTC were prepared in DMSO and diluted with media to give the desired concentrations. The final concentration of DMSO was kept at no more than 0.1% (v/v). Briefly, cells were grown in 75-cm^3 flasks to about 90% confluency, trypsinized, washed with ice-cold PBS and resuspended in serum-free RPMI medium at a cell density of 10^6 cells/ml. MDA-MB-231/R cells were incubated with various concentrations of aurones (0.05 μM, 0.5 μM, 5 μM) or vehicle (0.1% DMSO in RPMI) at 37 °C for 15 min, followed by the addition of MX (3 μM) for 30 min. FTC, a specific inhibitor of BCRP, was tested at 10 μM as a positive control. After the incubation period, ice-cold PBS (10 ml) was added to stop the process and the cells were removed by centrifugation (2000 rpm, 5 min, 4 °C). The cell pellet was washed with ice-cold PBS (3×) and resuspended in cold PBS for the determination of the intracellular concentration of MX on a FACScan flow cytometer (CyAn® Research Flow Cytometer, Dako, Glostrup, Denmark). Cells were excited at 488 nm and the emission recorded via a 680 nm long-pass filter for the detection of MX fluorescence. The data were analyzed with the instrument's software (Summit version 4.3, Dako, Glostrup, Denmark). MX levels in the cells were normalized to the vehicle control (0.1% DMSO) which was taken as 100%. At least three independent determinations were carried out for each test compound. MX accumulation in

the MDA-MB-231 cells was expressed by the following equation:

$$\text{MX accumulation (\%)} = \frac{\text{area}_{(\text{cells+test compound+MX})} - \text{area}_{(\text{cells})}}{\text{area}_{(\text{cells+MX})} - \text{area}_{(\text{cells})}} \times 100$$

2.5. Mitoxantrone sensitization

The ability of aurones to re-sensitize MDA-MB-231/R cells to MX was assessed by determining the growth inhibitory IC_{50} of MX in the presence of various concentrations of the test aurone. Stock solutions of MX, FTC and test aurones were prepared in DMSO and diluted with media so that final concentrations in the well did not exceed 1% (v/v) DMSO. Cells (10^4) were seeded in 96-well plates and incubated for 24 h, after which, the culture medium in each well was replaced with fresh medium containing various concentrations of MX and test aurone (0.05 μM or 0.5 μM). FTC (10 μM) was tested as positive control. After 72 h of incubation, the drug-containing medium was removed and cells were washed once with PBS. Hundred microlitres of 0.5 mg/ml MTT was then added to each well, incubated for 3 h at 37 °C, after which the MTT solution was decanted and DMSO (100 μl) was added to dissolve the purple formazan crystals. Absorbance was read at 590 nm on a microplate reader with at least three separate determinations made for each concentration of test compound. The absorbance values obtained at a known concentration of MX were averaged and adjusted by subtraction of absorbance of empty wells ("blank"). This value was expressed as a percentage of the average absorbance obtained from control wells (wells with cells and media containing 1% DMSO) which were also adjusted by subtraction of the blank to give % surviving cells. The IC_{50} value of MX was determined from the sigmoidal curve obtained by plotting % surviving cells at various concentrations of MX using GraphPad Prism (Version 4.00, GraphPad Software, San Diego, CA). The software used the four-parameter logistic equation given by the expression for determination of IC_{50}:

$$Y = \frac{\text{bottom} + (\text{top} - \text{bottom})}{(1 + 10^{(\log IC_{50} - X) \times \text{HillSlope})})},$$

where X is the logarithm of concentration and Y is the response.

2.6. Cytotoxicity studies

The cytotoxicity profiles of the aurones on different cell lines were determined by the MTT assay as described in Section 2.5. The cell lines tested were the human breast cancer cell line MDA-MB-231 (V and R), human colon carcinoma cell line HCT 116 and the normal human fibroblast CCL 186. Stock solutions of aurones were prepared in DMSO and diluted with media to give concentrations of 10 μM for investigations on MDA-MB-231 (V and R) cells, and 5 μM on the other two cell lines. The final concentration of DMSO in the well did not exceed 1% (v/v). Cell survival was determined as a % of control cells and at least two determinations were made for each concentration of aurone.

2.7. Uptake of calcein-AM in MDCK/MDR1 cells

A previously described method was followed with some modifications (Liu et al., 2008). Briefly, MDCKII/MDR1 and MDCKII/WT cells were grown to 80–90% confluency, trypsinized and seeded in 96-well plates at a cell density of 2.5×10^4 cells/well. After incubation at 37 °C for 24 h, a monolayer of cells was obtained at the bottom of the well. The medium was decanted and the monolayer carefully washed with PBS. Stock solutions (10 mM) of test compounds were prepared in DMSO and diluted with Hank's buffered saline solution (HBSS) such that addition of an aliquot (100 μl) gave a final concentration of 10 μM test compound in the well. The final concentration of DMSO in each well did not exceed 1% (v/v). After incubation for 30 min (37 °C, 5% CO_2 atmosphere), calcein-AM in HBSS–DMSO (100 μl) was added to each well to give a final concentration of 2 μM. Incubation was continued for another 10 min, after which fluorescence was measured at 10 min intervals for 50 min on a microplate reader with $\lambda_{\text{excitation}}$ of 485 nm and $\lambda_{\text{emission}}$ of 535 nm. Concurrent determinations were made for the positive controls verapamil and cyclosporin A, both at 10 μM. The accumulation of calcein-AM was calculated at the 50th minute using the following equation:

$$\text{calcein-AM accumulation (\%)} = \frac{F_{\text{MDCKII/MDR1+test compound}}}{F_{\text{MDCKII/MDR1}}} \times 100$$

2.8. Molecular modeling

Structures of aurones were drawn and geometry minimized using the Hamiltonian forcefield MMFF94x in MOE® (Chemical Computing Group, Montreal, Canada). The following molecular descriptors were collected for the aurones using the QuaSAR module of MOE®: constitutive (number of rotatable bonds, hydrogen bond donors, hydrogen bond acceptors), lipophilic (calculated log P in oil/water), geometric (van der Waals surface area of hydrogen bond acceptors and hydrogen bond donors, total hydrophobic van der Waals surface area, topological polar surface area) and electronic (sum of atom polarizabilities). These descriptors are given in Table 1 of Supplementary Information The software was also used to determine distances and angles between rings and hydrogen bond donor groups in selected energy-minimized compounds. Principal component analysis (PCA) and projection to latent structures by partial least squares analysis (PLS), available on SIMCA-P 11 (Umetrics AB, Umea, Sweden), were used to develop structure–activity relationships.

2.9. X-ray crystallography

Crystals of 5-hydroxy-2-(4′-methoxybenzylidene)-benzofuran-3(2*H*)-one and aurone **8** were grown in methanol and dichloromethane solutions, respectively and mounted on glass fibres. X-ray data were collected with a Bruker AXS SMART APEX diffractometer, using Mo Kα radiation at 223 K, with the SMART suite of Programs (*SMART* version 5.628 (200), Bruker AXS Inc., Madison, WI). Data were processed

and corrected for Lorentz and polarization effects with SAINT (*SAINT+* version 6.22a (2001) Bruker AXS Inc., Madison, WI), and for absorption effect with SADABS (*SADABS*, version 2.10 (2001), University of Göttingen). Structural solution and refinement were carried out with the SHELXTL, suite of programs (*SHELXTL*, Version 6.14 (2000), Bruker AXS Inc., Madison, WI). The structure was solved by direct methods to locate the heavy atoms, followed by difference maps for the light, non-hydrogen atoms. All non-hydrogen atoms were generally given anisotropic displacement parameters in the final model whereas H-atoms were placed at calculated positions.

2.10. *Statistical analysis*

Data were analyzed for statistically significant differences using one-way ANOVA followed by a Dunnett's post hoc test (SPSS 15.0 for Windows, Chicago, IL). p-Values <0.05 were considered statistically significant.

3. Results

3.1. *Synthesis of aurones (1–15)*

The structures of the synthesized aurones (**1–15**) are given in Table 1. These aurones had methoxy groups at positions 4 and 6 of ring A and differed only in the type of substituent on ring B. The choice of methoxy groups on the ring A was prompted by the docking results of Schoepfer et al. who showed that a functionalized 4,6-dihydroxaurone interacted with the ATP-binding site of CDK2 by hydrogen bonding via the 4-hydroxy and carbonyl groups (Schoepfer et al., 2002). Introducing methoxy in place of hydroxyl groups would minimize interactions with the ATP-binding sites of CDK2 and related proteins, and possibly reduce unwanted interactions. Moreover, Hadjeri and co-workers identified 4,6-dimethoxyaurone as an outstanding modulator of Pgp-mediated multidrug resistance, which showed that methoxy groups did not adversely affect, and may even increase affinity for the transport protein (Hadjeri et al., 2003).

Table 1 – Structures of 4,6-dimethoxyaurones (1–15)

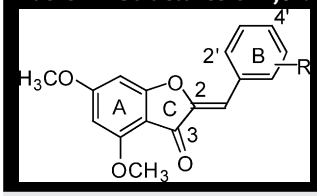

Compound	R
1	H
2	2′-Cl
3	3′-Cl
4	4′-Cl
5	2′-OH
6	3′-OH
7	4′-OH
8	2′-OCH_3
9	3′-OCH_3
10	4′-OCH_3
11	2′-CH_3
12	3′-CH_3
13	4′-CH_3
14	3′-CN
15	4′-CN

The substituents (chloro, methoxy, hydroxy, methyl, cyano) were selected based on their different locations on the Craig Plot (Craig, 1971). Hence, substituents with a range of lipophilic and electron withdrawing/donating effects were represented in this series. Each substituent was attached to three different positions (2′, 3′ or 4′) on ring B, with the exception of the cyano group where only two regioisomers (3′, 4′) were prepared.

The 4,6-dimethoxyaurones were synthesized following previous reports (Beney et al., 2001; Lawrence et al., 2003) and the key steps are illustrated in Scheme 1. The first step (Step a) involved the synthesis of 3,5-dimethoxyphenoxyacetic acid (**16**) by a hydride-catalyzed condensation of 3,5-dimethoxyphenol with chloroacetic acid. The product was subjected to intramolecular cyclization via Friedal–Craft acylation (Step b) to form the benzofuran-3-one ring which was then reacted with various benzaldehydes in a base-catalyzed aldol reaction to give the target aurones in moderate yields.

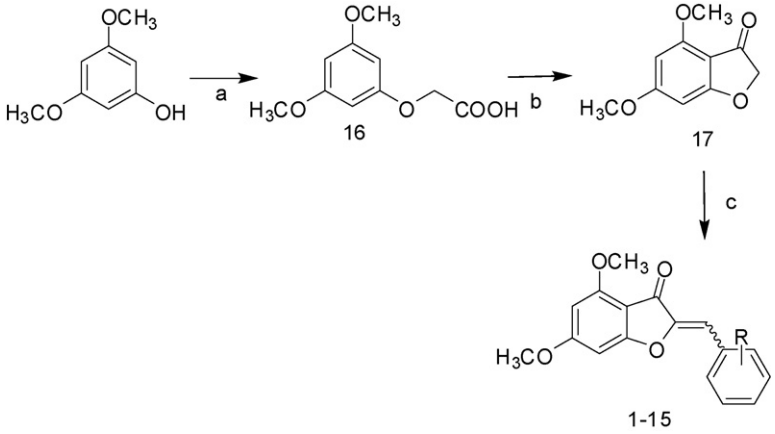

Scheme 1 – General procedure for the synthesis of 4,6-dimethoxyaurones. Reagents and conditions: (a) chloroacetic acid, NaH, DMF, rt, 12 h. (b) Polyphosphoric acid, 80 °C, 8 h. (c) Substituted benzaldehyde, 50% KOH in MeOH/H_2O, rt, 3 h.

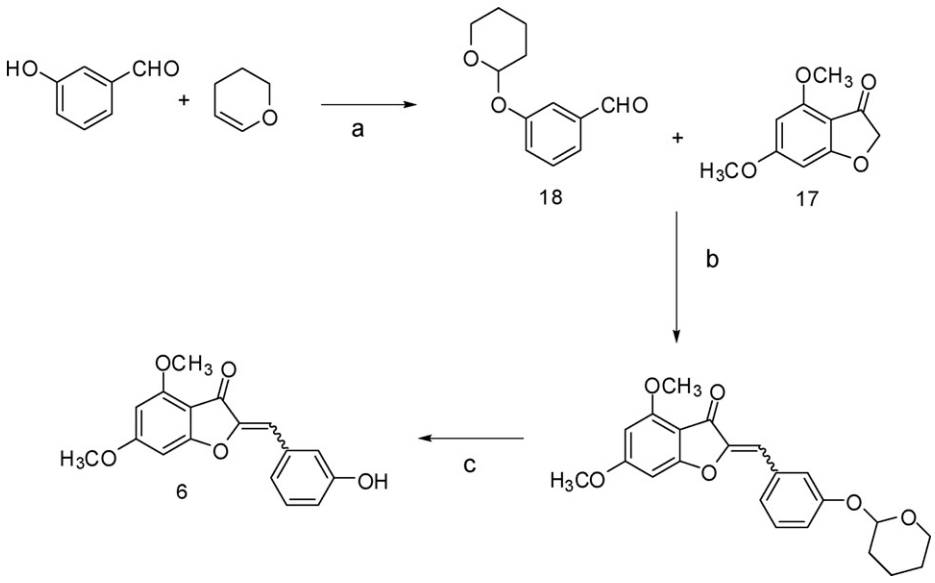

Scheme 2 – Protection and deprotection of phenolic hydroxyl group on 3′-OH benzaldehyde for synthesis of aurone 6. Reagents and conditions: (a) pyridinium *p*-toluenesulphonate (0.2 mmol), CH_2Cl_2, rt, 4 h. (b) 50% KOH in MeOH/H_2O, rt, 3 h.(c) 4 M HCl, rt, 4 h.

For aurones **6** and **7**, the reacting benzaldehyes (3 and 4-hydroxybenzaldehydes) required protection of their phenolic hydroxyl groups by conversion to the tetrahydropyranyl ether prior to condensation with **17**. Thereafter, the protecting moiety was removed by acid hydrolysis to give the desired hydroxylated aurones **6** and **7** (Scheme 2). Protection was not necessary for 2-hydroxybenzaldehyde.

3.2. *Assignment of configuration of aurones*

The 4,6-methoxyaurones may exist as either *E* (*trans*) or *Z* (*cis*) isomers, with the *Z* isomer generally regarded as the thermodynamically more stable form (Ur-Rahman et al., 2001) Many authors have made the *Z*/*E* assignment of aurones based on the chemical shift of the olefinic (β) proton (Beney et al., 2001; Thakkar and Cushman, 1995; Okombi et al., 2006). The olefinic proton in the *E* isomer is deshielded to a greater extent than the same proton in the *Z* isomer and hence has a larger chemical shift. In the literature, a chemical shift of δ 6.70 ppm was cited for the *Z* isomer and δ 7.01 ppm for the *E* isomer (Beney et al., 2001; Thakkar and Cushman, 1995). *Z*/*E* isomers were also distinguished by the ^{13}C chemical shift of the exocyclic carbon (=CH) (Pelter et al., 1979). In the *Z* isomer, the chemical shift was reported at δ 111 ppm while in the *E* isomer, it was observed at a higher frequency of δ 120–130 ppm.

Both ^{13}C and ^{1}H chemical shifts were considered for the assignment of the *Z*/*E* configuration of the aurones. The ^{13}C chemical shifts of the exocyclic carbon in all compounds appeared at δ 105–111 ppm, in keeping with a Z configuration of the exocyclic double bond. However, there was some ambiguity when the ^{1}H chemical shifts of the β hydrogen were considered. Most of the aurones had values in the range of δ 6.68–6.77 ppm, consistent with reported values for known Z aurones. On the other hand, aurones with 2′-substituents (**2**, **5**, **8**, **11**) had values of δ 7.00–7.38 ppm, which implied the presence of an *E* configuration. Thus, the configuration of the 2′-substutituted aurones could not be unequivocally assigned based on chemical shifts alone. In order to resolve the problem, the X-ray structure of aurone **8** (2′-methoxy on ring B) in the solid state was examined (Fig. 1a). It was found to have the *Z* configuration and this led us to assign the same configuration to the remaining 2′-substituted aurones. The X-ray structure of another aurone, 5-hydroxy-2-(4′-methoxybenzylidene)-benzofuran-3(2*H*)-one that was not included in the present series, was also available (Lee, unpublished results). This aurone had a 4′-methoxy substituent on ring B and a chemical shift of δ 6.87 ppm for its β hydrogen. As anticipated, the X-ray analysis showed that it had a *Z* configuration. Thus, spectroscopic and crystallographic data supported the assignment of a *Z* configuration for the aurones. The down field shift of the β hydrogen observed for the 2′-substituted aurones may be due to the anomalous "ortho effect" often associated with such substituents.

3.3. *Effect of aurones on cell survival of MDA-MB-231, HCT116 and CCL-186 cells*

The aurones were evaluated for antiproliferative activity on human breast cancer cells that were transfected with the plasmid vector carrying human wild type ABCG2 (MDA-MB-231/R) or the empty vector plasmid (MDA-MB-231/V). The presence of ABCG2 in MDA-MB-231/R cells was verified by Western blot analysis. ABCG2 was not detected in the MDA-MB-231/V cells (Fig. 2). The cell model was also investigated for the expression of other transport proteins (ABCB1, ABCC1, and ABCC2) and these were not detected (data not shown).

When tested at 10 μM against MDA-MB-231/V and R cells, some aurones were found to be slightly more potent against V cells than R cells. These were **2**, **4**, **6**, **8** which at 10 μM caused about 30–85% survival of V cells but 100% survival of R cells.

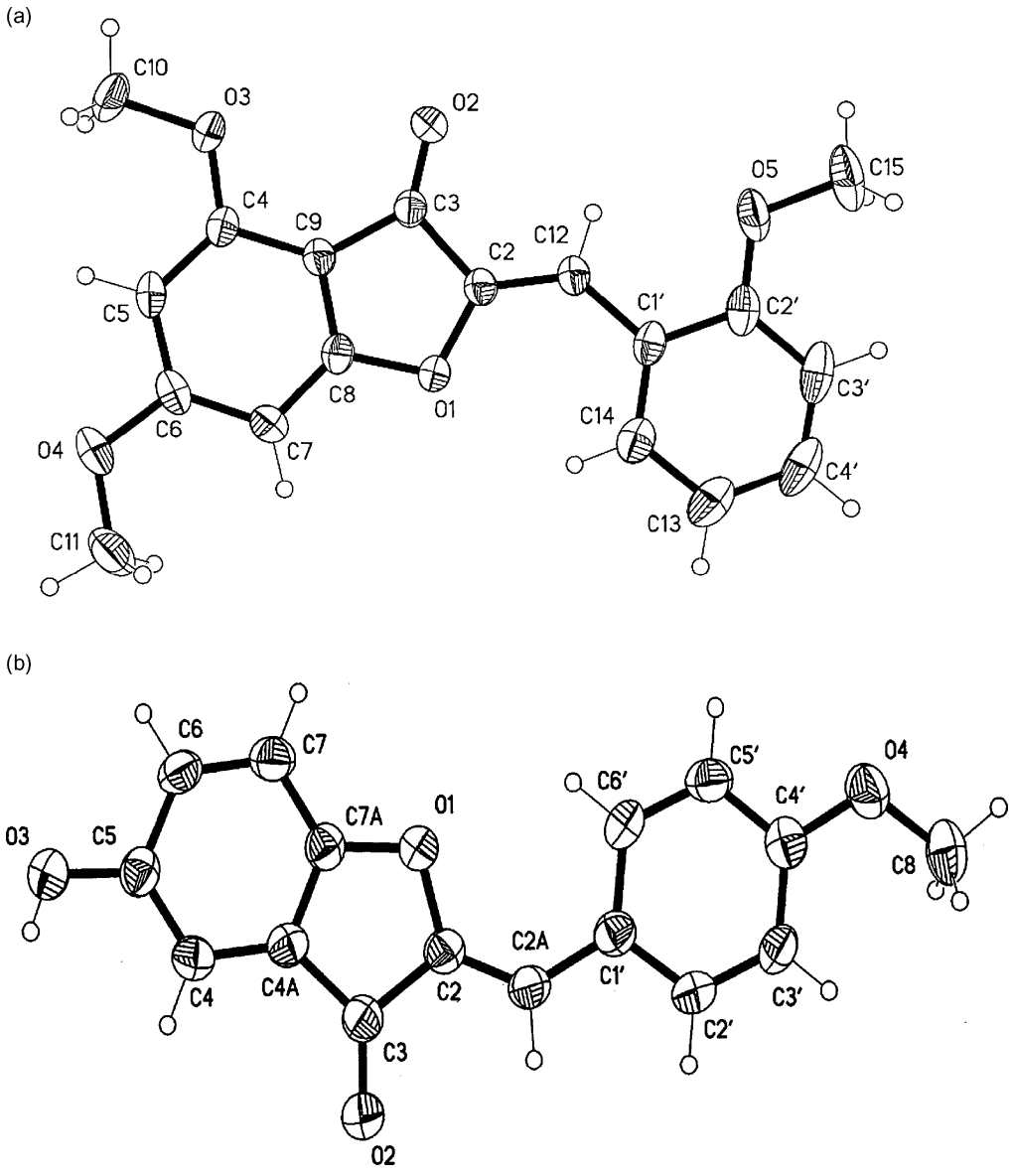

Fig. 1 – Molecular structures of (a) 4,6-dimethoxy-2-(2′-methoxybenzylidene)-benzofuran-3(2*H*)-one (8) and (b) 5-hydroxy-2-(4′-methoxybenzylidene)-benzofuran-3(2*H*)-one, showing the Z configuration of the exocyclic double bond.

Aurone **2** had the greatest cytotoxic effect on V cells, with 37% cell survival at 10 μM and 62% survival at 5 μM. However, only two determinations were made for these compounds against the V cells and would require further confirmation.

Fig. 2 – Western blot analyses of ABCG2 in MDA-MB-231 (R and T) cells. [a]Analyses of ABCG2 expression in MDA-MB-231/R and MDA-MB-231/V cells. The protein loading for each sample was 15 μg as determined by protein assay. [b]β-Actin was used as a positive control for the Western blot analyses.

To determine if the effects were tissue- or tumour-specific, the aurones (except **11**, **12**, **14**) were tested at 5 μM against a colon cancer cell line (HCT116) and a normal cell line (CCL186). All the aurones had limited activity (>80% cell survival) against the normal cell line but affected the survival of HCT116 cells to a greater extent, with aurones **2** and **3** associated with particularly low levels of cell survival (37%, 50%). Aside from these compounds, the other aurones showed limited antiproliferative activity against the panel of four cell lines (Table 2).

3.4. *Effect of aurones on the efflux of mitoxantrone from ABCG2-expressing MDA-MB-231 cells*

Mitoxantrone is a substrate of ABCG2 and accumulates to a lesser extent in the ABCG2 expressing MDA-MB-231/R cells than non-ABCG2 expressing MDA-MB-231/V cells. In our hands, V cells accumulated 2.4-fold more MX than R cells.

Table 2 – Effects of aurones on percentage cell survival in various cell lines[a]

Compound	R	% Cell survival			
		MDA-MB-231/R 10 μM	MDA-MB-231/V 10 μM	HCT116 5 μM	CCL 186 5 μM
1	H	122 (9)	101	76	>100
2	2′-Cl[b]	115	37	27	93
3	3′-Cl	103 (16)	102	50	>100
4	4′-Cl	126 (21)	87	60	>100
5	2′-OH	115 (16)	101	56	>100
6	3′-OH	105 (11)	83	93	97
7	4′-OH	114 (8)	156	94	>100
8	2′-OCH_3	126 (31)	86	67	88
9	3′-OCH_3	112 (12)	133	74	>100
10	4′-OCH_3	136 (16)	122	80	92
11	2′-CH_3	116 (32)	134	ND[c]	ND[c]
12	3′-CH_3	83 (32)	90	ND[c]	ND[c]
13	4′-CH_3	116 (40)	120	81	>100
14	3′-CN	113 (8)	158	ND[c]	ND[c]
15	4′-CN	108 (7)	179	94	>100

[a] Cell survival (%) = (average absorbance of wells with test compounds at 590 nm/average absorbance of wells with medium and 1% DMSO) × 100. Values are mean of two or more independent determinations. S.D. in parenthesis for $n = 3$ determinations.
[b] Percentage cell survival in MDA-MB-231/V cells for compound **2** at 5 μM = 62%, mean of two independent determinations.
[c] ND, not determined.

The accumulation of MX in R cells was determined in the presence of three different concentrations of test aurone (5 μM, 0.5 μM, 0.05 μM) (Table 3). The results showed that the extent of MX accumulation varied according to the concentration used. Aurones tested at 0.05 μM had no significant effect on MX accumulation. When the concentration was increased to 0.5 μM, 10 aurones increased MX accumulation to a significant extent ($p < 0.05$) compared to untreated cells and at a higher concentration of 5 μM, 11 members caused significant MX accumulation. Thus, a large number of the aurones were effective at 0.5 μM and they caused accumulation of MX to levels comparable to that of the known ABCG2 inhibitor FTC which was tested at a higher concentration of 10 μM.

Table 3 – Accumulation of MX in MDA-MB-231/R cells in presence of aurones

Compound	R	MDA-MB-231/R MX accumulation (% of control)[a]		
		Aurone concentration		
		5 μM	0.5 μM	0.05 μM
	Control (0.1% DMSO)		100	
	FTC (10 μM)		237 (60.9)*[b]	
1	H	283 (86.6)*	209 (32.7)*	150 (5.1)
2	2′-Cl	275 (62.9)*	226 (22.6)**	148 (30.3)
3	3′-Cl	275 (55.3)*	231 (30.9)**	160 (20.9)
4	4′-Cl	233 (23.8)	195 (44.0)	125 (8.7)
5	2′-OH	235 (50.5)	214 (29.9)*	131 (16.3)
6	3′-OH	273 (65.5)*	235 (29.1)**	139 (11.1)
7	4′-OH	263 (54.3)*	219 (26.7)*	138 (23.5)
8	2′-OCH_3	251 (46.8)	217 (25.1)*	148 (18.2)
9	3′-OCH_3	294 (70.9)**	222 (31.9)*	169 (18.0)
10	4′-OCH_3	278 (57.1)*	215 (30.1)*	146 (21.8)
11	2′-CH_3	321 (146)**	163 (53.6)	72.6 (24.0)
12	3′-CH_3	291 (46.2)**	203 (60.2)*	117 (14.1)
13	4′-CH_3	268 (48.7)*	130 (27.1)	88.8 (13.8)
14	3′-CN	358 (64.7)***	172 (40.5)	117 (29.4)
15	4′-CN	187 (39.6)	161 (50.9)	81.0 (31.4)

[a] MX accumulation (% of control) in MDA-MB-231/R cells calculated as: MX accumulation (% of control) (%) = $[\text{area}_{(\text{cells+test compound+MX})} - \text{area}_{(\text{cells})}/\text{area}_{(\text{cells+MX})} - \text{area}_{(\text{cells})}] \times 100$. Values are expressed as mean of two or more independent determinations. S.D. in parenthesis for $n = 3$ determinations.
[b] Significant difference (*$p < 0.05$, **$p < 0.01$, ***$p < 0.001$) between MX accumulation in the presence of test aurone and control (0.1% DMSO) (one-way ANOVA followed by Dunnett post hoc test).

Western blots showed that MDA-MB-231/R cells had no detectable levels of ABCB1, ABCC1 or ABCC2 expression. Therefore the increase in MX accumulation in MDA-MB-231/R cells was ascribed to the inhibition of ABCG2 by the aurones. To further confirm this point, the effect of aurones at 5 μM was investigated in MDA-MB-231/V cells that were not transfected with ABCG2. It was found that levels of accumulation were not different from those observed in untreated control V cells (Supplementary Information, Table 2). Therefore, the higher levels of MX accumulation in the R cells resulted from the inhibition of ABCG2 activity by the aurones.

3.5. *Effect of selected aurones (3,6,9,14) on the IC_{50} of mitoxantrone in MDA-MB-231/R cells*

In order to confirm the functional relevance of the aurone-induced increase in MX accumulation in MDA-MV-231/R cells, selected aurones (**3**, **6**, **9**, **14**) were tested for their ability to restore MX sensitivity to the ABCG2 expressing MDA-MV-231/R cells. **3**, **6** and **9** were chosen because of their good outcomes in the MX accumulation assays, and **14** was selected as a negative control as it had a lesser effect on MX accumulation (Table 3). Re-sensitization was assessed by determining the effect of a fixed concentration of aurone on the IC_{50} of MX on MDA-MB-231/R cells. In the absence of aurones, the IC_{50} values of MX were 0.09 μM (V cells) and 3.45 μM (R cells) (Table 4). The 38-fold difference in IC_{50} values was ascribed to ABCG2 which extruded MX from R cells but not V cells. The IC_{50} of MX was reassessed in the presence of either 0.05 μM or 0.5 μM aurone. At these concentrations, the aurones did not adversely affect cell survival, as described in Section 3.2. FTC at 0.05 and 0.5 μM were included as positive controls. A representative curve for the IC_{50} determination of MX in the presence of aurone **3** is given in Fig. 3.

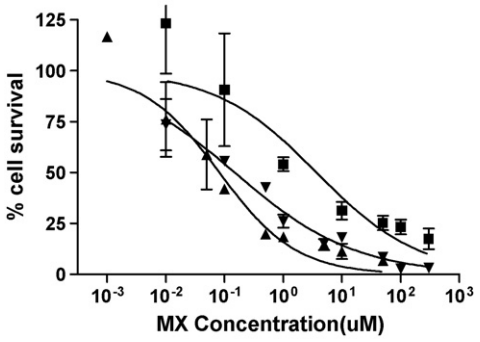

Fig. 3 – IC_{50} determinations of mitoxantrone (MX) in parental MDA-MB-231/V cells (▲), MDA-MB-231/R cells (■), MDA-MB-231/R cells in presence of 3 (0.5 μM) (▼).

A statistical comparison of the IC_{50} values of MX in untreated R cells (no aurone) and treated R cells (with aurone) showed a significant lowering of the IC_{50} of MX at both aurone concentrations (0.5 μM, 0.05 μM) ($p < 0.05$). At the higher concentration of 0.5 μM, the aurones caused more than 10-fold increase in MX potency, with aurones **3** and **9** associated with a 23–25-fold increase. At this concentration, the aurones were also more effective than FTC in restoring sensitivity of the cells to MX. It was noted that aurone **14** which was meant to be the negative control also re-sensitized the R cells to MX.

The effect of the aurones on the fold resistance index of MX on the R and V cell lines was also considered. In the absence of aurones, the fold resistance index of MX on the two cell lines was 38($IC_{50\ MX(R\ cells)}$/$IC_{50\ MX(V\ cells)}$), which meant that MX was 38 times less sensitive on the transfected R cells compared to the parental V cells. With FTC (0.5 μM), the difference in sensitivity was reduced to sevenfold, but with aurones **3** and **9**, the index was further reduced to 1.6–1.7. It is likely that when tested at a higher concentration, these aurones would restore MX to its original sensitivity against V cells.

Table 4 – Effect of selected aurones on IC_{50} of mitoxantrone in MDA-MB-231/R cells

Compound	R	IC_{50} of mitoxantrone (μM)[a,b]	
		MDA-MB-231/R	Fold resistance index[c]
Control		3.45 (1.34)	(3.45/0.09 = 38.3)
0.05 μM			
3	3′-Cl	1.67 (0.52)[d]*	18.5
6	3′-OH	1.77 (0.67)*	19.7
9	3′-OCH_3	1.11 (0.19)*	12.3
14	3′-CN	0.95 (0.27)**	10.6
	FTC	0.87 (0.22)**	9.7
0.5 μM			
3	3′-Cl	0.14 (0.07)***	1.6
6	3′-OH	0.26 (0.10)***	2.9
9	3′-OCH_3	0.15 (0.04)***	1.7
14	3′-CN	0.30 (0.17)***	3.3
	FTC[e]	0.67	7.4

[a] IC_{50} values are presented as mean of two or more independent determinations. S.D. in parenthesis for $n = 3$ determinations.
[b] IC_{50} value of MX in MDA-MB-231/V cells = 0.09 (0.07) μM.
[c] Fold resistance index to MX = IC_{50} of MX in R cells$_{(absence\ or\ presence\ of\ aurone)}$/$IC_{50}$ of MX in V cells.
[d] Significant difference (*$p < 0.05$, **$p < 0.01$, ***$p < 0.001$) between IC_{50} of MX in the presence of test aurone and the absence of test aurone (control) in MDA-MB-231/R cells (one-way ANOVA followed by Dunnett post hoc test).
[e] IC_{50} value of MX in MDA-MB-231/R cells in the presence of FTC at 10 μM = 0.33 μM determined from duplicate determinations.

3.6. *Effect of aurones on the accumulation of calcein-AM in MDCKII/MDR1 cells*

The aurones were investigated at 10 μM for their effects on the accumulation of calcein-AM, a ABCB1 substrate, by MDCKII cells transfected with ABCB1 (MDCKII/MDRI). Western blot analysis confirmed the presence of ABCB1 in these cells (Fig. 4). The parental cells (MDCKII/WT) showed constitutive levels of ABCB1 but at lower levels compared to the transfected cell line.

Calcein-AM is non-fluorescent until it is taken up by cells where it is hydrolyzed by enzymes to give calcein which fluoresces. Thus, the accumulation of calcein-AM is assessed from the intensity of fluorescence and inhibitors of ABCB1 will cause an increase in the fluorescence intensity. In this experiment, known ABCB1 inhibitors—cyclosporin A and verapamil (both at 10 μM) were used as controls and they increased

Fig. 4 – Western blot analyses of ABCB1 in MDCK II/MDR1 and MDCK II/WT cells. [a]Analyses of ABCB1 expression in MDCKII/MDR1 and MDCKII/WT cells. The protein loading for each sample was 40 μg as determined by protein assay. [b]β-Actin was used as a positive control for the Western blot analyses.

fluorescence intensity as anticipated. The accumulation of calcein-AM was also monitored in parental MDCK II cells and a ninefold difference was detected between the parental and transfected cell lines, with more calcein-AM accumulated in the parental MDCK II cells. Unlike the MX accumulation assay, the aurones were tested at a relatively high concentration of 10 μM on the calcein-AM assay. The choice of this concentration was to allow comparisons to be made with verapamil. In our hands, verapamil caused a significant increase in calcein-AM accumulation (300%) at 10 μM. Lower concentrations would cause smaller increases which would hamper comparisons with the test aurones. As it turned out, none of the aurones were significantly better than verapamil even at 10 μM (Table 5) although several (**3**, **6**, **9**, **10**, **12**, **13**, **14**) increased calcein-AM to the same extent as verapamil.

Table 5 – Accumulation of calcein-AM in MDCKII/MDR1 cells in the presence of aurones

Compound[a]	R	Calcein-AM accumulation (% of control)[b]
	MDCKII/MDR1 (control)	100
	MDCKII/MDR1 (verapamil)	301 (30.2)[c] ***
	MDCKII/MDR1 (cyclosporin A)	1000 (76.0)***
1	H	182 (7.87)
2	2′-Cl	108 (1.48)
3	3′-Cl	242 (21.3)***
4	4′-Cl	137 (6.26)
5	2′-OH	107 (5.27)
6	3′-OH	209 (30.1)**
7	4′-OH	121 (9.89)
8	2′-OCH_3	122 (11.1)
9	3′-OCH_3	303 (55.6)***
10	4′-OCH_3	294 (15.7)***
11	2′-CH_3	111 (4.26)
12	3′-CH_3	362 (61.0)***
13	4′-CH_3	255 (65.7)***
14	3′-CN	245 (47.6)***
15	4′-CN	126 (9.57)

[a] Determined at 10 μM test compound at the 50th minute. Values are expressed as mean of $n = 3$ determinations. S.D. given in parenthesis.

[b] Calcein-AM accumulation (%) = $[F_{MDCKII/MDR1 + test\ compound}]/[F_{MDCKII/MDR1}] \times 100$.

[c] Significant difference (**$p < 0.01$, ***$p < 0.001$) between calcein-AM accumulation in the presence of test aurone and control (0.1% DMSO) (one-way ANOVA followed by Dunnett post hoc test).

3.7. *Structure–activity relationships*

A comparison of inhibitory trends among aurones based on the levels of MX and calcein-AM accumulation (at 0.5 μM and 10 μM test aurone, respectively) showed some interesting differences between these two activities. First, aurone **1** with no substituent on ring B significantly increased MX but not calcein-AM accumulation, which would suggest that a substituted ring B was less important for inhibition of ABCG2 as compared to ABCB1. Second, several aurones with 3′-substitutents (**3**, **6**, **9**, **12**) were associated with better ABCB1 inhibitory activities than their respective 2′ and 4′ regioisomers. Such a trend was not seen with ABCG2 inhibition. Third, a larger number of aurones significantly increased MX accumulation at 0.5 μM (Table 3) as compared to calcein-AM accumulation (Table 5), even though a higher concentration of aurone was used for the latter. Lastly, there was some indication from the data that aurones with good ABCG2 inhibitory activity were poor ABCB1 inhibitors and vice versa. Aurones **1**, **2**, **5**, **7**, **8** were significantly better ABCG2 inhibitors (0.5 μM, compared to control, $p < 0.05$) but these same aurones were no better than the control when evaluated as ABCB1 inhibitors (Tables 3 and 5). In the case of aurones **13** and **14**, they were better inhibitors of ABCB1 than ABCG2, but when **14** was subsequently tested for re-sensitization of MBA-MB-231/R cells to MX, it fared just as well as the other active aurones (**3**, **6**, **9**). This may imply that there are limitations in using a non-concentration related dependent variable (like MX accumulation at a fixed concentration) for analysis.

In order to have a better understanding of these structure–activity trends, a quantitative structure–activity analysis was attempted. Descriptors that encompassed constitutive, geometric, lipophilic and electronic characteristics were collated and used in the analysis. ABCG2 inhibitory activity was expressed in terms of MX accumulation (normalized to 100%) at 0.5 μM test compound, and ABCB1 inhibitory activity (normalized to 100%) was expressed in terms of calcein-AM accumulation at 10 μM test compound. PCA and projection to latent structures by PLS were attempted but both approaches did not provide meaningful models for interpretation. Possible reasons may be the limited number of compounds in this series, their restricted structural diversity, and the absence of a concentration term (like EC_{50} for increasing MX or calcein-AM accumulation to 50% of the maximum) as dependent variables for the analysis.

Matsson and co-workers (2007) proposed a three point pharmacophore for inhibitors of ABCG2 which comprised of two hydrophobic features and one hydrogen (H) bond acceptor function. This model was derived from 28 structurally heterogenous ABCG2 inhibitors and characterized by specified distances and angles. We were interested to evaluate the fit of the aurones on this model in view of their ABCG2 inhibitory activity. Aurone **3** was chosen as a representative member and two other chalcones (**20** and **21**) that were tested for ABCG2 inhibitory activity in our laboratory were also assessed. Chalcone **20** at 0.5 μM re-sensitized MDA-MB-231/R cells to MX with a fold resistance index of 8.5 (Han et al., 2008) while chalcone **21** had no effect on MX accumulation in ABCG2-overexpressing MCF-7 cells (Liu et al., 2008). Although the three compounds were tested in our laboratories

Table 6 – Distances and angles of the pharmacophoric triangle for aurone 3 and chalcones 20, 21

	Mattson et al.	Aurone 3[b]	Chalcone 20[b]	Chalcone 21[b]
Distances (Å) between pharmacophore points[a]				
Ring A–Ring B	6.74	6.76	7.53	7.53
Ring A–HBA	3.47	2.76	2.75	2.75
Ring B–HBA	9.84	8.62	10.04	10.04
Angles (°) at each pharmacophore point[a]				
Ring A	146.9	124.1	151.7	151.7
Ring B	11.1	15.4	7.5	7.5
HBA	22.0	40.5	20.9	20.9

The dimensions reported by Matsson et al. (2007) are included for comparison.

[a] Measured from energy minimized structures drawn on MOE® (CCG, Montreal, Canada). The centroids of rings A and B were used for measurements involving the rings.

[b] Rings A, B and hydrogen bond acceptor (in brackets) in aurone **3** and chalcones **20** and **21**. The 6-OCH_3 and 4-OH groups in aurone **3** and the chalcones gave the best fit distances to the model proposed by Matsson et al. (2007)

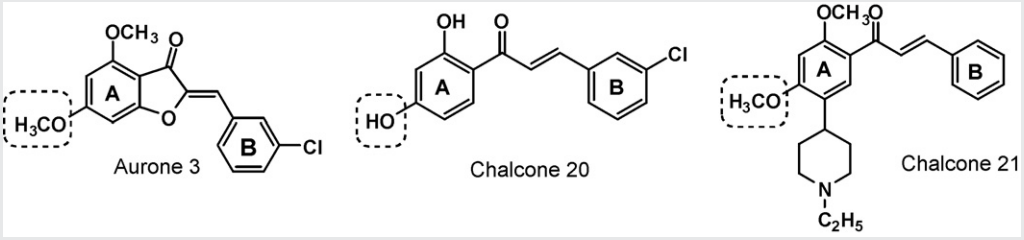

at different times and using assays that were not completely similar, it is reasonable to rank their ABCG2 inhibitory properties in the order of aurone **3** > chalcone **20** > chalcone **21**. The hydrophobic rings and H bond acceptor groups in each compound are indicated in Table 6, alongside the relevant distances and angles. Since more than one H bond acceptor group was present in each compound, the group that complied best with the reported distances was chosen. A depiction of the pharmacophore points in aurone **3** is given in Fig. 5.

It is seen that the distance between the hydrophobic rings (A, B) in aurone **3** complied with the optimal distance in the pharmacophore model (6.76 Å vs. 6.74 Å), but the other two distances (ring B-HBA, ring A-HBA) deviated from the proposed values. The distances in the two chalcones (**20**, **21**) were almost identical and quite different from those found in aurone **3**. In particular, the distances between the hydrophobic rings in the chalcones (7.53 Å) were greater than the same distance in the aurone (6.76 Å) and the pharmacophore model (6.74 Å). On the other hand, the distances between ring B and

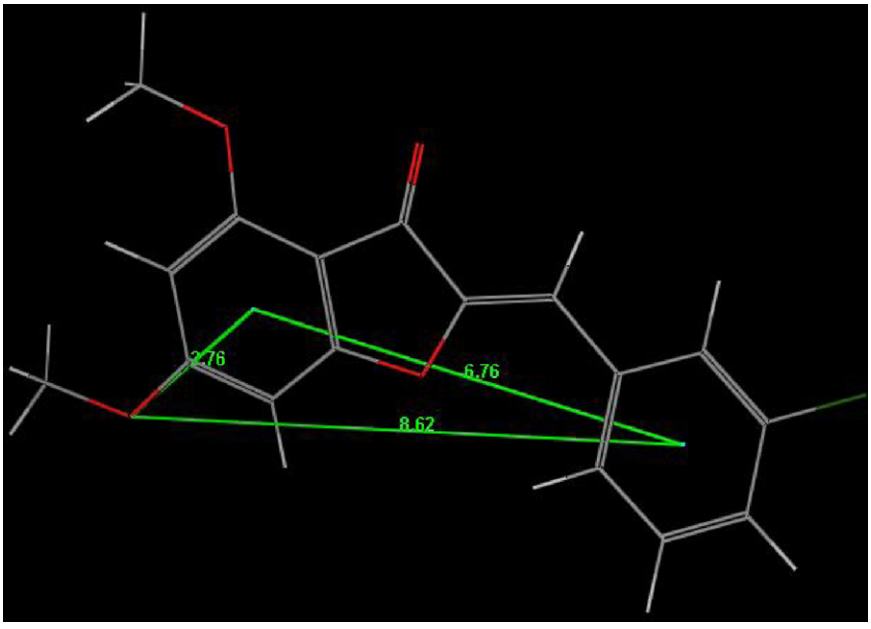

Fig. 5 – Depiction of hydrophobic rings (A, B) and H bond acceptor (6-OCH_3) group in aurone 3. Distances are in Å units and measured by MOE.

the H bond acceptor in the chalcones (10.04 Å) were closer to the distance (9.84 Å) in the model. Similarly, the angles in the pharmacophore model and the test compounds showed varying degrees of compliance. Neither the aurones nor the chalcones showed a convincing fit to the reported pharmacophore model. Comparison of distances and angles showed that the two chalcones were identical in spite of their differing activities as ABCG2 inhibitors.

4. Discussion

Several 4,6-dimethoxyaurones increased the accumulation of the MX in MDA-MB-231/R cells which were transfected with ABCG2. These cells did not show detectable levels of other transporters (ABCB1, ABCC1, ABCC2) in immunoblotting experiments. The aurones did not increase MX accumulation in MDA-MD-231/V cells that were not transfected with ABCG2. These findings were consistent with the inhibition of the ABCG2 efflux transporter. The aurones increased MX accumulation at 0.5 μM and they were more potent than FTC which brought about the same level of accumulation but at a higher concentration (10 μM). Several aurones were found to re-sensitize MDA-MB-231/R cells to MX, with some members (**3**, **9**) reducing the difference in sensitivities between transfected (R) and parental (V) cell lines to a mere twofold at 0.5 μM. The aurones were again more effective than FTC (0.5 μM) in restoring MX sensitivity to MDA-MB-231/R cells.

The good ABCG2 inhibitory activity of the aurones was complemented by their low antiproliferative activity on cultured cell lines, as shown from the high levels of survival of cancerous (MBA-MB-231/R, MBA-MB-231/V, HCT 116) and non-cancerous (CCL 186) cell lines exposed to fixed concentrations (5 μM or 10 μM) of most aurones. Although growth inhibitory IC_{50} values were not determined in this investigation, values exceeding 10 μM can be expected. The weak antiproliferative activities of the aurones were in sharp contrast to those reported by Lawrence et al. (2003) which had submicromolar IC_{50} values against a human myelogenous leukemia cell line (K562). Those aurones were heavily methoxylated on both rings A and B and the most promising compound had four methoxy groups, with three on ring A. In comparison, the present series of aurones had only two methoxy groups on ring A. It may be that antiproliferative activity is influenced by the number of methoxy groups attached to the benzofuranone ring of the aurone. Unfortunately, the aurones were not more cytotoxic on the MDA-MB-231/R cells that overexpressed ABCG2 than the MDA-MB-231/V cells. This would have been a very desirable feature because the aurones could then overcome drug resistance by eliminating the ABCG2 overexpressing cells. A thiosemicarbazone NSC73306 was reported to selectively kill Pgp expressing multidrug resistant cancer cells besides inhibiting ABCG2 efflux activity (Wu et al., 2007).

It was observed that some aurones (**2**, **4**, **6**, **8**) were more cytotoxic against the parental MDA-MB-231/V cells than the transfected R cells, raising the possibility that these compounds may be ABCG2 substrates. These compounds would then be actively extruded by ABCG2 in the transfected R cells, resulting in lower cytotoxicity. Imatinib (Lemos et al., 2008), dipyridamole (Y. Zhang et al., 2005), the thiosemicarbazone NSC73306 (Wu et al., 2007) were reported to have dual substrate and inhibitor profiles. The possibility of aurones functioning as dual ABCG2 substrates and inhibitors warrants further investigation as it would have important implications on their modulatory properties. One approach would be to investigate how these compounds affected ABCG2-mediated ATP hydrolysis. The ability of ABCG2 and ABCB1 to extrude agents out of cells is driven by ATPase activity and ATP production. Substrates would be expected to increase ATPase activity and enhance ATP production while inhibitors would have the opposite effect. The reality however may be less straightforward. For example, pheophorbide A, a substrate of ABCG2 had a biphasic effect on ABCG2 ATPase activity, stimulating ATP hydrolysis at lower concentrations but inhibiting ATP hydrolysis at higher concentrations (Wu et al., 2007). Curcumin stimulated ABCG2 ATPase activity even though it was cited as an inhibitor of ABCG2 (Chearwae et al., 2006).

ABC transport modulators can either bind and compete with substrate binding at the substrate binding site(s) or interfere with ATP binding or hydrolysis by binding to the ATP-binding site. Photoaffinity labeling of ABCG2 with different photoaffinity analogues would provide a useful means of distinguishing between these interactions. [^{125}I] Iodoarylazidoprazosin, a photoaffinity analogue of prazosin, has been used to characterize the substrate binding sites of ABCG2 (Shukla et al., 2006). If aurones are substrates, they would inhibit the photolabeling of ABCG2 with this reagent. On the other hand, the photoaffinity ATP analogue [α-^{32}P] 8-azidoATP binds specifically to the nucleotide binding domains of numerous ABC transporters and it may be used, alongside the ATPase assay, to test if aurones interacted with the ATP-binding site of ABCG2 (Wu et al., 2007).

A meaningful QSAR could not be derived from the available data but qualitative deductions on structural trends were evident. The most important observation related to the different structural requirements for inhibition of the two transport proteins, even for a relatively simple template like the aurones. The benzylidene ring B was less critical for ABCG2 inhibition. An unsubstituted ring B had as much inhibitory effect as one that was substituted with groups of different lipophilicities and electron donating/withdrawing properties. This was not the case for ABCB1 inhibition where substitution of ring B was important, with greater inhibition associated with substitution at the 3′ position. The nature of the group (lipophilic or hydrophilic, electron donating or withdrawing) at 3′ was however less critical. These different requirements would imply that aurones were either good inhibitors of ABCG2 or ABCB1, but not both. This was indeed noted for several aurones but would require further validation with a larger number of compounds.

The 4,6-dimethoxyaurone template was also compared to a reported pharmacophore model for ABCG2 inhibitors. Of the three distances in the reported model, only the distance between the hydrophobic rings (A and B) of the aurone showed a good fit. On the other hand, a chalcone with no ABCG2 inhibitory activity also showed compliance but to a different distance in the model. The inference was that some distances in the model may be more critical than others and based on the three test compounds and their relative potencies as ABCG2

inhibitors, this may be the distance between the hydrophobic rings.

In summary, this study has demonstrated the potential of the 4,6-dimethoxy aurones as inhibitors of ABCG2. Aurones were found to re-sensitize ABCG2 expressing cancer cells to MX at submicromolar concentrations and to exhibit low antiproliferative activity against several cell lines. Different structural requirements were observed for aurones that were good inhibitors of ABCG2 or ABCB1, implying that appropriate changes in structure may give rise to aurones with selectivity for one protein. If subsequent investigations provide further support for the latter, aurones may have considerable utility in advancing the understanding of ABCG2 function.

Acknowledgements

We wish to thank Dr. Douglas D. Ross (Greenebaum Cancer Center, University of Maryland, Baltimore, USA) for the generous gift of MDA-MB-231 (R and V) cells, and Dr. Anton Berns (Netherlands Cancer Institute, Antoni van Leeuwenhoek Hospital, Amsterdam, Netherlands) for his kind provision of MDCK II/MDR1 cells. This work was made possible by funding RP 148 000 084 112 to MLG, RP 148 050 078 101/133 to PLRE, and National University of Singapore graduate scholarships to HMS, CYL.

Appendix A. Supplementary data

Supplementary data associated with this article can be found, in the online version, at doi:10.1016/j.ejps.2008.07.008.

REFERENCES

Beney, C., Mariotte, A.-M., Boumendjel, A., 2001. An efficient synthesis of 4,6 dimethoxyaurones. Heterocycles 55, 967–972.

Boumendjel, A., 2003. Aurones: a subclass of flavones with promising biological potential. Curr. Med. Chem. 10, 2621–2630.

Boumendjel, A., Beney, C., Deka, N., Mariotte, A., Lawson, M., Trompier, D., Baubichon-Cortay, H., Di Pietro, A., 2002a. 4-Hydroxy-6-methoxyaurones with high-affinity binding to cytosolic domain of P-glycoprotein. Chem. Pharm. Bull. 50, 854–856.

Boumendjel, A., Di Pietro, A., Dumontet, C., Barron, D., 2002b. Recent advances in the discovery of flavonoids and analogs with high-affinity binding to P-glycoprotein responsible for cancer cell multidrug resistance. Med. Res. Rev. 22, 512–529.

Breedveld, P., Beijnen, J., Schellens, J., 2006. Use of P-glycoprotein and BCRP inhibitors to improve oral bioavailability and CNS penetration of anticancer drugs. Trends Pharmacol. Sci. 27, 17–24.

Chearwae, W., Shukla, S., Limtrakul, P., Ambudkar, S.V., 2006. Modulation of the function of the multidrug resistance-linked ATP-binding cassette transporter ABCG2 by the cancer chemopreventive agent curcumin. Mol. Cancer Ther. 5, 1995–2006.

Craig, N.P., 1971. Interdependence between physical parameters and selection of substituent groups for correlation studies. J. Med. Chem. 14, 680–684.

Hadjeri, M., Barbier, M., Ronot, X., Mariotte, A., Boumendjel, A., Boutonnat, J., 2003. Modulation of P-glycoprotein-mediated multidrug resistance by flavonoid derivatives and analogues. J. Med. Chem. 46, 2125–2131.

Han, Y., Riwanto, M., Go, M.L., Ee, P.L.R., 2008. Modulation of breast cancer resistance protein (BCRP/ABCG2) by non-basic chalcone analogues. Eur. J. Pharm. Sci. 35, 30–41.

Lawrence, N.J., Rennison, D., Mcgown, A.T., Hadfield, J.A., 2003. The total synthesis of an aurone isolated from *Uvaria hamiltonii*: aurones and flavones as anticancer agents. Bioorg. Med. Chem. Lett. 13, 3759–3763.

Lemos, C., Jansen, G., Peters, G.J., 2008. Drug transporters: recent advances concerning BCRP and tyrosine kinase inhibitors. Br. J. Cancer 98, 857–862.

Liu, X.L., Tee, H.W., Go, M.L., 2008. Functionalized chalcones as selective inhibitors of P-glycoprotein and breast cancer resistance protein. Bioorg. Med. Chem. 16, 171–180.

Matsson, P., Englund, G., Ahlin, G., Bergström, C., Norinder, U., Artursson, P., 2007. A global drug inhibition pattern for the human ATP-binding cassette transporter breast cancer resistance protein (ABCG2). J. Pharmacol. Exp. Ther. 323, 19–30.

Minderman, H., Suvannasankha, A., O'Loughlin, K., Scheffer, G., Scheper, R., Robey, R., Baer, M., 2002. Flow cytometric analysis of breast cancer resistance protein expression and function. Cytometry 48, 59–65.

Okombi, S., Rival, D., Bonnet, S., Mariotte, A., Perrier, E., Boumendjel, A., 2006. Discovery of benzylidenebenzofuran-3(2*H*)-one (aurones) as inhibitors of tyrosinase derived from human melanocytes. J. Med. Chem. 49, 329–333.

Ono, M., Maya, Y., Haratake, M., Ito, K., Mori, H., Nakayama, M., 2007. Aurones serve as probes of beta-amyloid plaques in Alzheimer's disease. Biochem. Biophys. Res. Commun. 361, 116–121.

Pare, P.W., Dmitrieve, N., Mabry, T.J., 1991. Phytoalexin aurone induced in cephalocereus senilis liquid suspension culture. Phytochemistry 30, 1133–1135.

Pelter, A., Ward, R.S., Heller, H.G., 1979. Carbon-13 nuclear magnetic resonance spectra of (*Z*)- and (*E*)-aurones. J. Chem. Soc., Perkin Trans. 1, 328–329.

Robert, J., Jarry, C., 2003. Multidrug resistance reversal agents. J. Med. Chem. 46, 4805–4817.

Schoepfer, J., Fretz, H., Chaudhuri, B., Muller, I., Seeber, E., Meijer, I., Lozach, O., Vangrevelinghe, E., Furet, P., 2002. Structure-based design and synthesis of 2-benzylidene-benzofuran-3-ones as flavopiridol mimics. J. Med. Chem. 45, 1741–1747.

Shukla, S., Robey, R.W., Bates, S.E., Ambudkar, S.V., 2006. The calcium channel blockers, 1,4-dihydropyridines, are substrates of the multidrug resistance-linked ABC drug transporter, ABCG2. Biochemistry 45, 8940–8951.

Shukla, S., Wu, C., Ambudkar, S., 2008. Development of inhibitors of ATP-binding cassette drug transporters: present status and challenges. Expert Opin. Drug Metab. Toxicol. 4, 205–223.

Szakács, G., Paterson, J., Ludwig, J., Booth-Genthe, C., Gottesman, M., 2006. Targeting multidrug resistance in cancer. Nat. Rev. Drug Discov. 5, 219–234.

Thakkar, K., Cushman, M., 1995. A novel oxidative cyclization of 2′-hydroxychalcones to 4,5-dialkoxyaurones by thallium(III) nitrate. J. Org. Chem. 60, 6499–6510.

Ur-Rahman, A., Choudhary, M.I., Hayat, S., Kahn, A.M., Ahmed, A., 2001. Two new aurones from marine brown alga spatoglossum variabile. Chem. Pharm. Bull. 49, 105–107.

Václavíková, R., Boumendjel, A., Ehrlichová, M., Kovár, J., Gut, I., 2006. Modulation of paclitaxel transport by flavonoid derivatives in human breast cancer cells. Is there a correlation between binding affinity to NBD of P-gp and modulation of transport? Bioorg. Med. Chem. 14, 4519–4525.

Wu, C., Shukla, S., Calcagno, A., Hall, M., Gottesman, M., Ambudkar, S., 2007. Evidence for dual mode of action of a thiosemicarbazone, NSC 73306: a potent substrate of the multidrug resistance linked ABCG2 transporter. Mol. Cancer Ther. 6, 3287–3296.

Zhang, S., Yang, X., Coburn, R.A., Morris, M.E., 2005. Structure activity relationships and quantitative structure activity relationships for the flavonoid-mediated inhibition of breast cancer resistance protein. Biochem. Pharmacol. 70, 627–639.

Zhang, Y., Gupta, A., Wang, H., Zhou, L., Vethanayagam, R.R., Unadkat, J.D., Mao, Q., 2005. BCRP transports dipyridamole and is inhibited by calcium channel blockers. Pharm. Res. 22, 2023–2034.